Photocatalytic Degradation of Ethylene Emitted by Fruits with TiO2 Nanoparticles

Article *in* Industrial & Engineering Chemistry Research · March 2011

DOI: 10.1021/ie1005756

CITATIONS
41

READS
708

5 authors, including:

Murid Hussain
COMSATS University Islamabad
78 PUBLICATIONS **1,106** CITATIONS
SEE PROFILE

Francesco Geobaldo
Politecnico di Torino
156 PUBLICATIONS **5,491** CITATIONS
SEE PROFILE

I&EC research
Industrial & Engineering Chemistry Research

ARTICLE

pubs.acs.org/IECR

Photocatalytic Degradation of Ethylene Emitted by Fruits with TiO_2 Nanoparticles

Murid Hussain, Samir Bensaid, Francesco Geobaldo, Guido Saracco, and Nunzio Russo*

Department of Materials Science and Chemical Engineering, Politecnico di Torino, Corso Duca degli Abruzzi 24, 10129 Torino, Italy

Department of Chemical Engineering, COMSATS Institute of Information Technology Lahore Campus, M. A. Jinnah Building, Defence Road, Off Raiwind Road, Lahore 54000, Pakistan

ABSTRACT: The photocatalytic degradation of ethylene (emitted by fruits) by novel TiO_2 nanoparticles (TNPs), at 3 °C, has been investigated to consider the possibility of its use for the cold storage of fruits. TNP exhibits a high specific surface area, a good anatase-to-rutile mixed phase ratio, and more surface OH groups than commercially available Degussa P 25, as characterized by nitrogen adsorption, static light scattering, energy dispersive X-ray spectroscopy, X-ray diffraction, Fourier transform infrared spectroscopy, and X-ray photoelectron spectroscopy. TNPs, tested in an ad-hoc designed Pyrex glass photocatalytic reactor, showed higher photodegradation activity of ethylene than Degussa P 25. The superior characteristics of TNPs, compared to Degussa P 25, might induce the adsorption of ethylene and water and the generation of OH groups which act as oxidizing agents on the TNP surface, leading to higher photocatalytic activity. In the absence of water the photocatalytic degradation of ethylene reduced significantly. Moreover, a positive effect was observed when UV light was converged on the catalyst and an increase in ethylene degradation was achieved when UV light converging pipes and lens were used.

1. INTRODUCTION

Ethylene (C_2H_4) is an odorless and colorless gas which exists in nature and is generated by human activities as a petrochemical derivative, transportation engine exhausts, and thermal power plants.[1,2] However, naturally it is produced by plant tissues and biomass fermentation and occurs along the food chain, in packages, in storage chambers, and in commercial big refrigerators.[3] The effect of ethylene on fruit ripening and vegetable senescence is of significant interest for the scientific community.

Ethylene confers both positive and negative effects during fruit ripening.[1] Among the positive effects, ethylene stimulates the ripening process of climacteric fruits (apples, apricots, avocados, bananas, peaches, plums, and tomatoes), resulting in desirable flavors, colors, and texture (quality characteristics). In these kinds of fruits, negative effects can be found during postharvest storage, due to an acceleration of the ripening process (overripe fruits), leading to fruit quality loss.[4−7] During the postharvest storage of fruits and vegetables, ethylene can induce negative effects such as senescence, overripening, accelerated quality loss, increased fruit pathogen susceptibility, and physiological disorders. Fruits, vegetables, and flowers have ethylene receptors on their surface. Their actuation promotes ethylene production by the fruit itself and accelerates its ripening and aging.[2] Thus, preventing postharvest ethylene action is an important goal.

Literature shows some conventional as well as commercial techniques and technologies to control the action of ethylene. The most common are ethylene scavengers, especially the potassium permanganate ($KMnO_4$) oxidizer.[8] However, $KMnO_4$ cannot be used in contact with food products due to its high toxicity. Ozone (O_3) is also an alternative oxidant,[9] but it is highly unstable and decomposes into O_2 in a very short time. Carbons and zeolites are used as ethylene adsorbers and play a key role in the control of ethylene.[3,10,11] This technique only transfers the ethylene to another phase rather than destroying it. Hence, additional disposal or handling steps are needed. There are also some other alternative, attractive, but expensive materials[12] or techniques,[13] but the problem is cost effectiveness.

Photocatalytic degradation of hazardous materials is one of the most desirable and challenging goals in the research of the development of environmentally friendly catalysts.[14,15] It involves the actual destruction of organic contaminants rather than just the transfer of a contaminant from one phase to another.

In the present work, we have focused on the use of novel TiO_2 nanoparticles (TNPs) photocatalyst for ethylene degradation in fruits and vegetable cold storage, at low temperature, with the help of the new fabricated photocatalytic reaction system. An efficient way of utilizing this photocatalyst, which has superior characteristics for the target application, has been developed. Materials characterizations have been performed through specific surface area analysis, X-ray diffraction (XRD), static light scattering (SLS), energy dispersive X-ray spectroscopy (EDX), Fourier transform infrared spectroscopy (FT-IR), and X-ray photoelectron spectroscopy (XPS) in order to analyze the reaction. The photocatalytic activity of the TNP has also been compared with that of Degussa P 25 TiO_2.

Special Issue: IMCCRE 2010

Received: March 10, 2010
Accepted: September 21, 2010
Revised: September 20, 2010
Published: October 7, 2010

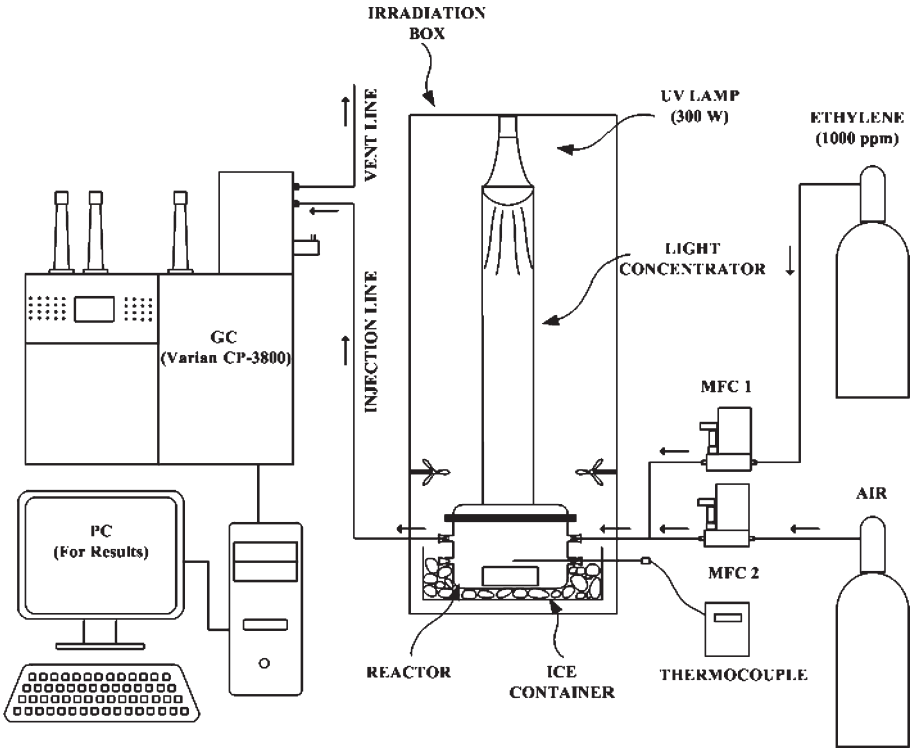

Figure 1. Ethylene photocatalytic reaction system.

2. EXPERIMENTAL SECTION

2.1. TNP Photocatalyst Synthesis. New TNPs were synthesized at a large scale (2 L of gel) by controlling the optimized operating parameters using the vortex reactor (VR) according to the procedure outlined in our previous work.[16] In details, two different solutions, one of titanium tetraisopropoxide (TTIP; Sigma-Aldrich) in isopropyl alcohol and the other of water (Milli-Q) in isopropyl alcohol were prepared separately under a nitrogen flux to control the alkoxide reactivity with humidity. Hydrochloric acid (HCl; Sigma Aldrich) was added to the second solution as a hydrolysis catalyst and deagglomeration agent. A TTIP/isopropyl alcohol concentration was taken as 1 M/L to obtain the maximum TiO_2 yield (1 M), $W([H_2O]/[TTIP]) = 4$, whereas the $[H^+]/[TTIP]$ ratio or H was set at 0.5. TTIP and water in isopropyl alcohol solutions were stored in two identical vessels and then pressurized at 2 bar with analytical grade nitrogen at inlet flow rates of 100 mL/min with two Rota meters. Equal volumes of reactant solutions (i.e., 1 L) were mixed at equal flow rates, at 25 °C, and the solutions exiting the VR were collected in a beaker thermostated at 25 °C and gently stirred. The obtained gel was then dried with a rotary evaporator. After complete drying at 150 °C overnight, the dried powder was eventually calcined at 400 °C for 3 h. The Degussa P 25 TiO_2 was purchased from Aerosil.

2.2. Characterization of the Photocatalyst. The Brunaer−Emmett−Teller (BET) specific surface area measurement was carried out on powders previously outgassed at 150 °C, by N_2 sorption at 77 K on a Quantachrome Autosorbe 1 C instrument. The XRD patterns were recorded on an X'Pert Phillips diffractomer using Cu Kα radiation, under the following conditions: 2θ = 10−90; 2θ step size = 0.02. Moreover, quantification of anatase:rutile phases was performed by X'Pert database library. The size distribution of the particles was measured by the SLS (Coulter LS 230), which was possible for particles ranging from 0.4 to 2000 μm. The SLS was also equipped with a polarization intensity differential scattering (PISD) device, which provided information in the 40−400 nm size range. The elemental composition of TNPs was checked by EDX analysis equipped with a high-resolution FE-SEM instrument (LEO 1525). The total UV light intensity was measured by Field Master Power Meter Head from COHERENT (Auburn, CA, USA) with a sensor of 3 cm inner diameter and capacity to measure from 10 mW to 100 W.

The nature of the OH groups was obtained with a Perkin-Elmer FT-IR spectrophotometer equipped with an MCT detector. The XPS spectra were recorded using a PHI 5000 Versa Probe with a scanning ESCA microscope fitted with an X-ray source of Al monochromatic (1486.6 eV, 25.6 W), a beam diameter of 100 μm, a neutralizer at 1.4 eV and 20 mA, and a FAT analyzer mode. All the binding energies were referenced to the C1s peak at 284.6 eV of the surface carbon. The individual components were obtained by curve fitting.

2.3. Ethylene Photocatalytic Reaction. The ethylene photocatalytic degradation was performed in a Pyrex glass reactor with a total volume of 2 L. A schematic of the experimental setup is depicted in Figure 1. The setup includes a Pyrex glass reactor (transparent to UV light) placed in ice at 3 °C, connectors, mass flow controllers (MFC, Bronkhorst high tech), a UV lamp (Osram ULTRA-VITALUX 300 W; has a mixture of light of UVA with a range of 320−400 nm and UVB with 290−320 nm wavelength which produces 13.6 and 3.0 W radiations, respectively; is ozone-free and radiations are produced by a mixture of quartz burner and a tungsten wire filament, as provided in manufacturer's information) with light converging pipes and lens, gas cylinders (1000 ppm ethylene, air), and a gas chromatograph (GC, Varian CP-3800) equipped with a capillary column (CP7381, fused silica) and a flame ionization detector (FID), which was used for the product gas analysis.

dx.doi.org/10.1021/ie1005756 |*Ind. Eng. Chem. Res.* 2011, 50, 2536–2543

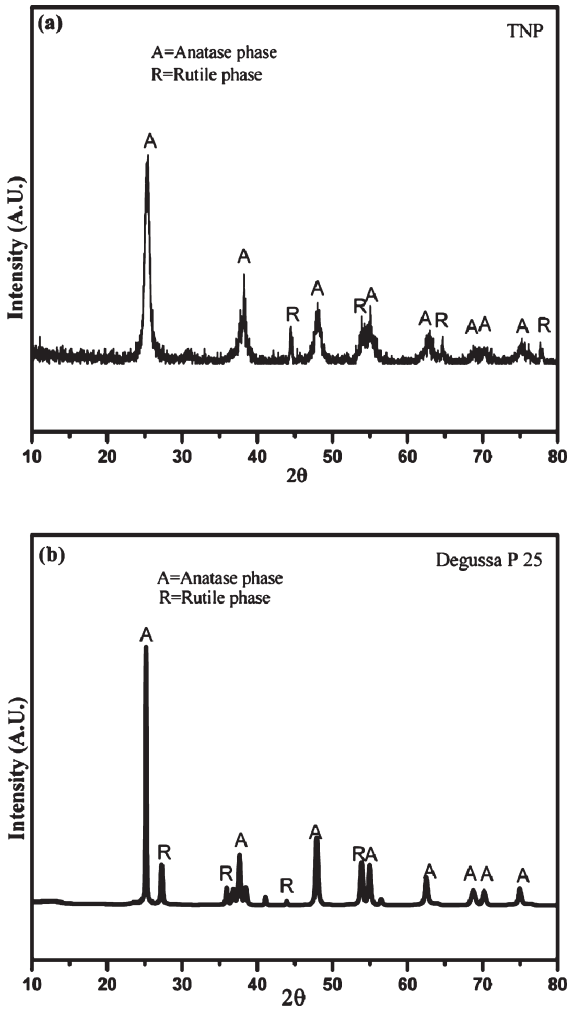

Figure 2. XRD patterns of (a) TNPs calcined at 400 °C/3 h and (b) commercial TiO_2 Degussa P 25.

A 1 g amount of the photocatalyst sample was spread homogeneously through hands inside the Pyrex glass reactor. A 100 ppm amount of ethylene was continuously flushed in the reactor, with the help of the MFC, at a constant flow rate of 100 mL/min. After achieving a steady-state in the peak intensity, the UV light was turned on and the reaction products were analyzed by GC. The degradation of ethylene C (%) was calculated as follows:

$$C = \frac{(C_i - C_o)}{C_i} \times 100$$

where C_i is the inlet concentration and C_o the outlet concentration of ethylene at steady state.

3. RESULTS AND DISCUSSION

3.1. Characteristics of TNP. The TNP, which was obtained by drying in a rotary evaporator and calcining at 400 °C/(3 h), showed a mixed anatase:rutile (80:20) phase,[16] as can be seen in Figure 2a. However, the Degussa P 25 also showed a mixed anatse:rutile (70:30) rutile phase but with a relatively larger rutile amount than the TNPs, as shown in Figure 2b with anatase (A) and rutile (R) peaks.

TNPs, as can be seen from the results of the BET analysis, have shown a larger specific surface area of 151 m^2/g and porosity.

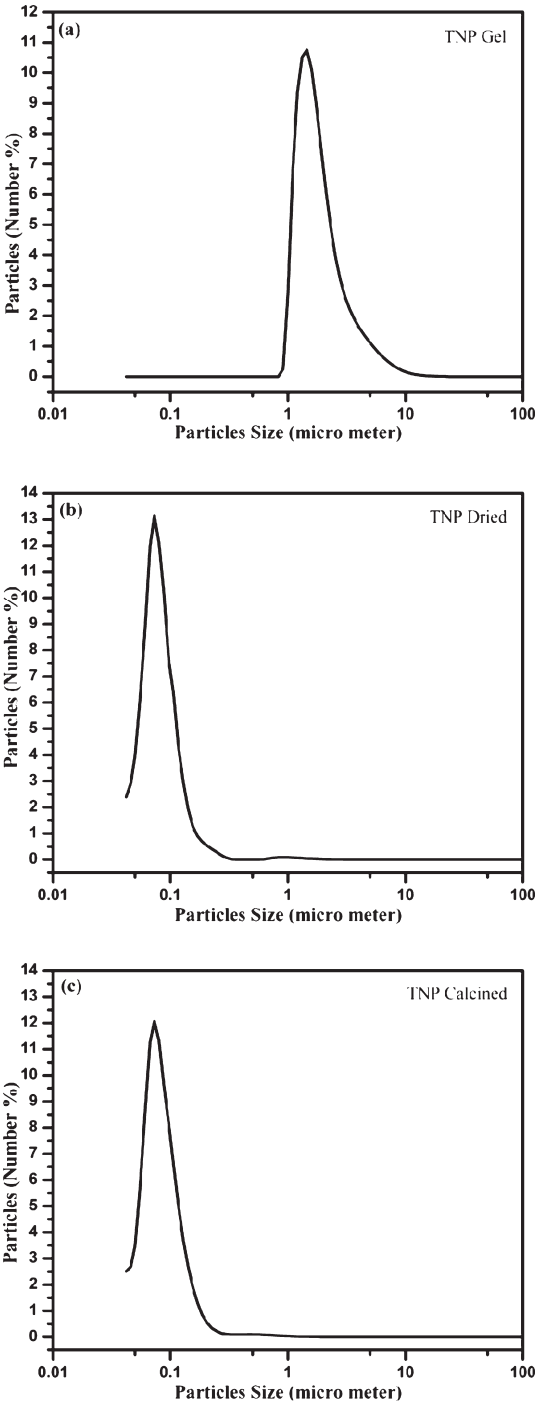

Figure 3. SLS results showing the number of particles and their size distribution: (a) TNP gel, (b) TNPs dried at 150 °C/overnight, and (c) TNPs calcined at 400 °C/(3 h).

Degussa P 25 has a three times smaller specific surface area, of 53 m^2/g, than TNPs, with a nonporous structure. Figure 3 shows the particle size distribution of the synthesized TNPs. It was found that a large number of particles were in the 1−10 μm range in the gel, as can be seen in Figure 3a. The TNP gel might show the aggregation of the small nanoparticles due to the presence of water. As the TNPs dried, a segregation of the particles took place due to the heat treatment and water evaporation, and the particles mostly showed a 40−100 nm size, as shown in

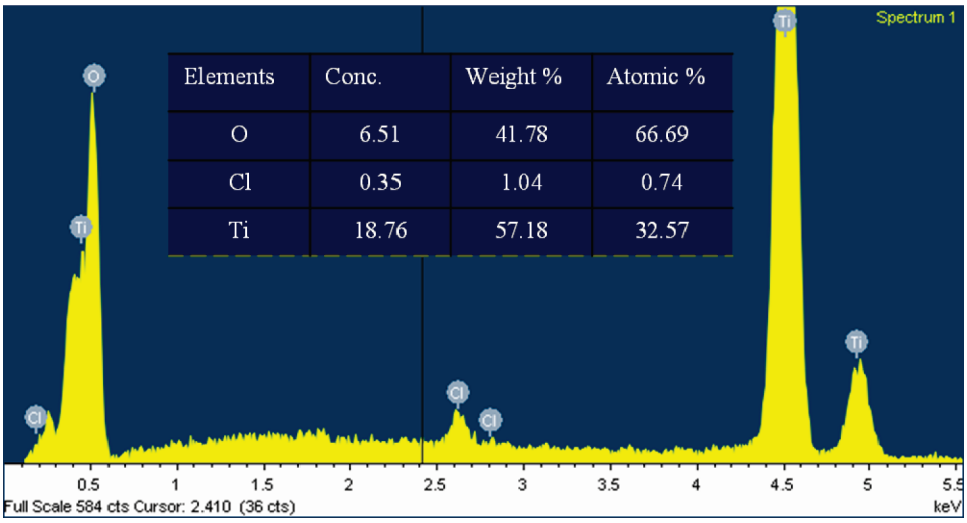

Figure 4. EDX analysis of TNPs.

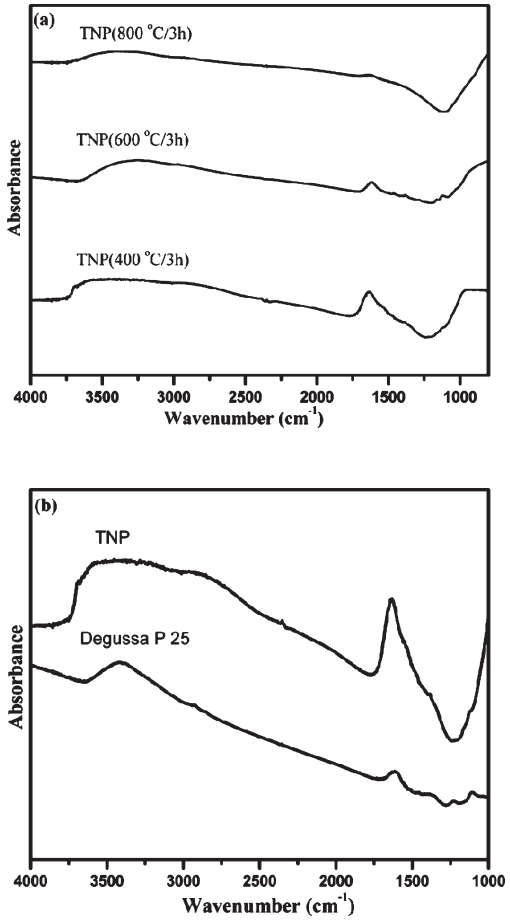

Figure 5. FT-IR absorbance spectra (a) after different calcination treatments of TNPs; (b) comparison of optimized TNPs and Degussa P 25, showing the difference in the surface OH groups.

Figure 3b. Similar results were also observed in Figure 3c for the dried powder after the high-calcination treatment of the TNP. These SLS results of the TNP were obtained by using the solutions of the respective dried powders in water. Hence, these are actually the secondary particles which might be formed by the aggregates of the primary particles in water. The primary particles of the calcined TNP powder were in the 10−20 nm range and those of the Degussa P 25 in the 60−80 nm range.[16]

Figure 4 shows the EDX analysis of the TNPs. This figure demonstrates that the main components are O and Ti with small Cl impurity. This Cl impurity is from the HCl that was added during the synthesis and is usually favorable for the photocatalytic reaction.[17]

The FT-IR spectra of the TNPs calcined at different temperatures, showing the difference in surface hydroxyl groups, are shown in Figure 5a. The broad peak centered at 3400 and the peak at 1650 cm^{-1} correspond to the surface-adsorbed water and hydroxyl groups. The increase in temperature to 800 °C significantly reduced the hydroxyl groups as a consequence of very small surface area (5 m^2/g) exposed. The FT-IR spectra of the optimized TNPs and the Degussa P 25 are shown in Figure 5b. The optimized TNPs, with a larger surface area than Degussa P 25, have in fact shown higher bands at 3400 and 1650 cm^{-1}.

3.2. Ethylene Photocatalytic Degradation. The photocatalytic degradation of ethylene was performed in the reaction system shown in Figure 1, at 3 °C, using ice, an artificial temperature atmosphere that is very close to that commonly used for the cold storage of fruits. Air was used instead of conventional oxygen for the photocatalytic reaction to obtain more representative data of practical application conditions, for commercialization purposes. Figure 6 shows the percentage degradation of ethylene as a function of illumination time at the low temperature of 3 °C, obtained using TNP and Degussa P 25 photocatalysts. After a preliminary saturation of the sample under the ethylene flow, there was no degradation in the dark in any of the experiments even in the presence of the catalyst or in the presence of UV light without the catalyst. Therefore, it can be concluded that the reaction results reported hereafter have only been photocatalytically induced.

Figure 6a shows the effect of surface hydroxyl groups on ethylene degradation. The ethylene degradation reduced very significantly as the surface hydroxyl groups decreased by increasing calcination temperature.

The optimized TNP photocatalyst has shown better ethylene degradation than the Degussa P 25 material (Figure 6b). This is due to the superior characteristics of the TNPs, the nanoparticles,

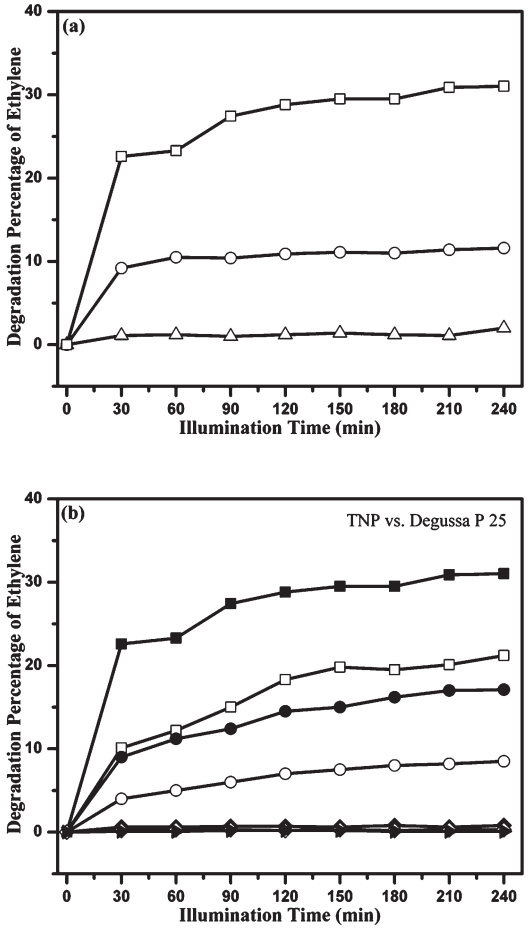

Figure 6. (a) Effect of OH groups on ethylene degradation at 100 ppm, 100 mL/min flow rate, 3 °C using ice, and 1 g of photocatalyst: (□) TNP(400°C/(3h))/UV lamp turned down to 75 cm; (○) TNP-(600°C/(3h))/UV lamp turned down to 75 cm; (Δ) TNP(800°C/-(3h))/UV lamp turned down to 75 cm. (b) Ethylene degradation over optimized TNP(400°C/(3h)) and Degussa P 25 photocatalysts at 100 ppm, 100 mL/min flow rate, 3 °C using ice, and 1 g of photocatalyst: (■) TNPs/UV lamp turned down to 75 cm; (□) Degussa P 25/UV lamp turned down to 75 cm; (●) TNPs/UV lamp turned up to 100 cm; (○) Degussa P 25/UV lamp turned up to 100 cm; (♦) TNPs/UV lamp turned off; (◊) Degussa P 25/UV lamp turned off; (right pointed filled triangle) no photocatalyst/UV lamp turned on.

the higher surface area, the amenable anatase-to-rutile phase ratio, and the larger amount of OH groups on the TNPs than on the Degussa P 25.

UV light intensity is an important factor in photocatalytic reactions.[18,19] Figure 6 shows this effect clearly when the UV lamp was kept low and the distance between the lamp and the reactor was 75 cm, compared to the initial 100 cm distance. The total UV intensity was increased to 57 mW/cm^2 at 75 cm compared to 35 mW/cm^2 at 100 cm distance. It can clearly be seen that the ethylene degradation is increased significantly due to the increased UV light intensity by lowering the lamp. It seems reasonable to conjunctive that the stronger the UV light intensity, the deeper the penetration of the UV light into the photocatalyst. Consequently, the degradation amount also increased.[18]

To utilize the UV light intensity in a positive way, light converging pipes and lens have been used to prevent UV light scattering and enhance its intensity in order to increase the

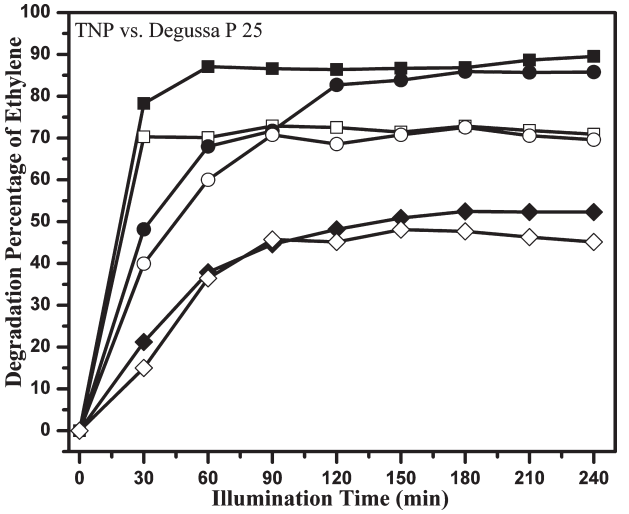

Figure 7. Ethylene degradation over TNPs and Degussa P 25 photocatalysts at 100 ppm, 100 mL/min flow rate, 3 °C using ice, and 1 g of photocatalyst: (■) TNPs/UV lamp turned down to 12 cm/(short converging pipe+lens); (□) Degussa P 25/UV lamp turned down to 12 cm/(short converging pipe+lens); (●) TNPs/UV lamp turned down to 12 cm/(short converging pipe); (○) Degussa P 25/UV lamp turned down to 12 cm/(short converging pipe); (♦) TNPs/UV lamp turned down to 87 cm/(tall converging pipe); (◊) Degussa P 25/UV lamp turned down to 87 cm/(tall converging pipe).

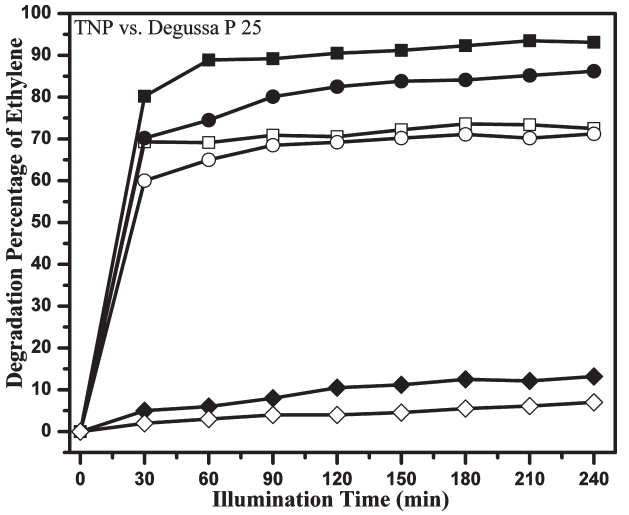

Figure 8. Water effect on ethylene degradation over TNPs and Degussa P 25 photocatalysts at 100 ppm, 100 mL/min flow rate, 3 °C using ice, and 1 g of photocatalyst, UV lamp turned down to 12 cm/(short converging pipe+lens): (■) TNP kept with 1 g of water for 12 h before reaction; (□) Degussa P 25 kept with 1 g of water for 12 h before reaction; (●) TNP fully dried in oven at 150 °C for 12 h and then kept with water for 12 h before reaction; (○) Degussa P 25 fully dried in oven at 150 °C for 12 h and then kept with water for 12 h before reaction; (♦) TNP fully dried in oven at 150 °C for 12 h and immediate reaction; (◊) Degussa P 25 fully dried in oven at 150 °C for 12 h and immediate reaction.

ethylene degradation. Figure 7 shows the effect of the converging pipes and the lens on the ethylene degradation at a low temperature. It has been observed that by lowering the UV lamp to a level of 87 cm and then converging the UV light by the tall

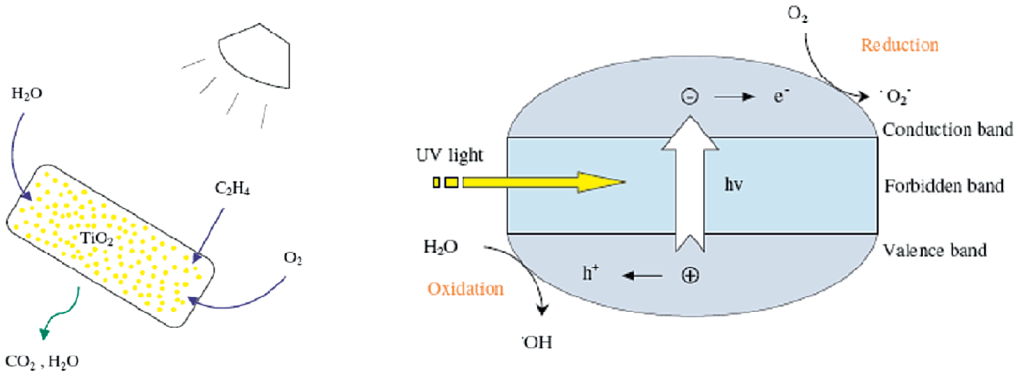

Figure 9. Ethylene photocatalytic reaction mechanism over TNPs.

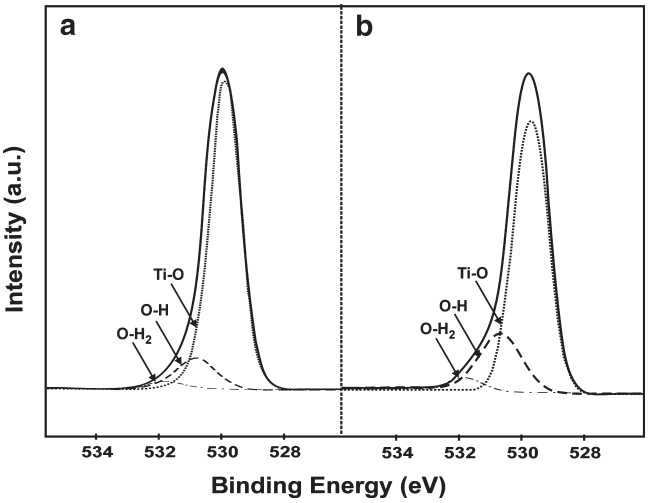

Figure 10. XPS analysis showing the OH and O−H_2 comparison by O1s: (a) Degussa P 25; (b) TNPs.

converging pipe (87 cm) significantly increased the ethylene degradation (Figure 7) due to the increased total UV light intensity (740 mW/cm^2), in comparison to the case without the pipe (Figure 6). A further increase in the degradation was obtained by lowering the lamp to 12 cm and using the small converging pipe (12 cm) where the total UV light intensity was increased to 2476 mW/cm^2. The TNP photocatalyst again showed a better performance than the Degussa P 25 due to its superior characteristics.

It has also been seen that the light converging pipes have significantly improved the ethylene degradation. The scattered UV light was only converged to the TiO_2 reaction part using the short and the tall converging pipes. It has also been observed that there is a gradual increase in the ethylene degradation as the illumination time increases, due to the low temperature at which the production of OH is comparatively more problematic than at room temperature. After attaining the required level of the OH groups, the degradation becomes constant. This effect was further studied using the combined form, the short converging pipe, and the lens, in order to obtain better results due to the further increase in the total UV light intensity (2548 mW/cm^2). It has been observed by Figure 7 that the combined effect significantly improved the gradually increasing trend in degradation to the maximum stable limit even after the initial illumination time. TNPs, as usual, again showed a better performance than Degussa P 25.

It has been observed that water has a significant effect on the photocatalytic degradation of ethylene, as shown in Figure 8. After complete drying of the titania, the ethylene degradation reduced significantly. It becomes very low at the initial illumination time due to a lack of water to proceed the reaction. However, there is a little improvement with the passage of illumination time which might be due to the water produced during reaction. This was confirmed when the fully dried titania was kept in a closed vessel with water for 12 h. After 12 h contact time, the titania showed much higher activity compared to the fully dried samples. However, there was a little improvement in ethylene degradation by keeping the normal titania with water. In all of these cases TNPs showed better ethylene degradation than Degussa P 25 which might be due to the higher surface area of TNPs for adsorption of water and ethylene.

Figure 9 shows the reaction mechanism of the TNP photocatalyst for ethylene photodegradation. The first main step should be the adsorption of water, O_2, and ethylene on the surface of the TNPs, followed by the formation of hole−electron pairs which need sufficient energy to overcome the band gap between the valence band (VB) and the conduction band (CB). The TNP catalyst derives its activity from the fact that when photons of a certain wavelength hit its surface, electrons are promoted from the valence band and transferred to the conductance band. This leaves positive holes in the valence band, which then react with the hydroxylated surface to produce $OH^{\bullet}$ radicals, the true oxidizing agents. In the absence of a suitable electron and hole scavengers, the stored energy is dissipated in a few nanoseconds through recombination. If a suitable scavenger or a surface defect state is available to trap the electron or hole, their recombination is prevented and a subsequent redox reaction may occur.[15] The synergistic effect of the anatase−rutile mixed phase in the TNP material, which is similar to the Degussa P 25 one, acts as a scavenger. The conduction band electron of the anatase part jumps to the less positive rutile part, reducing the recombination rate of the electrons and the positive holes in the anatase part. These $^{\bullet}OH$ and $^{\bullet}O_2^-$, which are produced, further react with ethylene to produce carbon dioxide and water[20] through the following overall equation:

$$C_2H_4 + 3O_2 \rightarrow 2CO_2 + 2H_2O$$

TNPs have shown a better activity than Degussa P 25 because they have several superior characteristics. They have small nanoparticles with a higher surface area and porosity than the nonporous Degussa P 25.[16] TNPs has a more amenable anatase-to-rutile ratio (80:20) compared to Degussa P 25. Moreover,

dx.doi.org/10.1021/ie1005756 |*Ind. Eng. Chem. Res.* 2011, 50, 2536–2543

Table 1. Atomic Concentrations (%) of TiO_2 Using XPS

catalyst	O1s	$Ti2p_{3/2,1/2}$	Ti−O	O−H	$O-H_2$	Ti^{3+}	Ti^{4+}
Degussa P 25	69.87	30.13	86.61	11.10	2.29	8.93	91.07
TNP	70.57	29.43	72.03	22.59	5.38	17.77	82.23

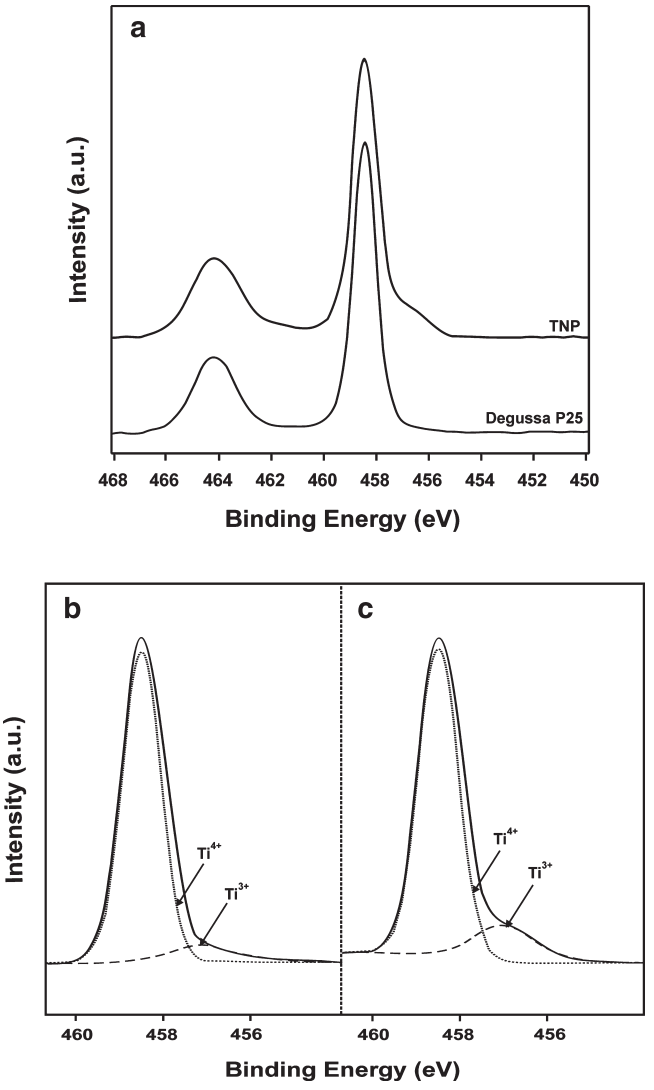

Figure 11. XPS analysis showing the comparison between $Ti2p_{3/2}$ and $Ti2p_{1/2}$ (a), and the Ti species comparison: (b) Degussa P 25; (c) TNPs.

TNPs have more surface OH groups than Degussa P 25, which might play a major role at low-temperature ethylene conversion. A further confirmation is therefore here provided from the results of the direct XPS measurements that were conducted to evaluate the hydroxyl groups and the evolution of the valence state of titanium on the TiO_2 surfaces. Figure 10 shows the oxygen O1s XPS spectra and the deconvolution results of TNPs and Degussa P 25 from a quantitative point of view. The O1s spectrum displayed peaks at 529.6 eV associated with Ti−O bonds in TiO_2, at 530.8 eV, which correspond to the hydroxyl Ti−OH,[21,22] whereas, at 532 eV, it shows $Ti-OH_2$,[23]23 which can be observed in the XPS spectra in Figure 10 (a, Degussa P 25; b, TNPs). TNPs clearly show more OH groups and OH_2 on the surface than Degussa P 25. The quantitative results are given in Table 1. The mass fraction of O1s, the hydroxyl groups, and the water of the two samples were calculated from the results of the curve fitting of the XPS spectra for the O1s region. The O1s values for the TNP and Degussa P 25 were 70.57 and 69.87%, respectively, and are similar. However, the O−H species for TNPs (22.59%) and Degussa P 25 (11.10%) are different. The water attached with Ti for TNPs (5.38%) and Degussa P 25 (2.29%) is also comparable. The higher OH groups on the surface of the TNPs than Degussa P 25 might play a major role in obtaining superior photocatalytic activity in ethylene photodegradation at low temperature.

Comparison of Ti2p spectra for TNPs and Degussa P 25 shows $Ti2p_{3/2}$ peak at 458.5 and $Ti2p_{1/2}$ at 464 eV, as shown in Figure 11a. However, the Ti species peaks, which are at binding energies of 456.7 (Ti^{3+}) and 458.5 eV (Ti^{4+}),[21] are shown in Figure 11 for Degussa P 25 (b) and TNPs (c). It is clear that TNPs have more Ti^{3+} species than Degussa P 25. After proper calculation through curve fitting, Table 1 shows that the TNP and Degussa P 25 catalysts have similar Ti2p values, but different Ti species. The TNP material has 17.77% Ti^{3+}, while Degussa P 25 only shows 8.93%. The Ti^{3+} species are responsible for oxygen photoadsorption, which results in the formation of O^-_{ads}, and which, together with the OH radical, is essential for photocatalytic oxidation.[24−26] The presence of surface Ti^{3+} causes distinct differences in the nature of the chemical bonding between the adsorbed molecule and the substrate surface.

4. CONCLUSIONS

TNP photocatalyst has successfully been used for the degradation of ethylene during tests conducted in an ad-hoc designed Pyrex glass photocatalytic reactor with a controlled atmosphere at low temperatures for commercial cold storage application. The TNP showed higher ethylene degradation results than the conventional Degussa P 25 photocatalyst. Besides the amenable anatase-to-rutile mix phase, the higher surface OH groups and more Ti^{3+} species, the small nanoparticles of the TNP with porosity showed large specific surface area which was three time higher than Degussa P 25. The large surface area of TNP helped to enhance the adsorption of water and ethylene to proceed the photocatalytic degradation. In the absence of water the photocatalytic degradation of ethylene was significantly reduced. Specifically designed pipes and lens helped to produce the required surface OH groups by converging UV light efficiently at the reaction place, and this in turn significantly enhanced the degradation of ethylene. The TNP photocatalyst has produced encouraging results in this study and has shown characteristics and the ability to be efficiently used for the degradation of ethylene produced in the cold storage of fruits. The proposed method with TNP for the ethylene photodegradation is simple and potentially economical to be applied commercially. Further research in this field would be useful.

AUTHOR INFORMATION

Corresponding Author

*Tel.: +39-011-0904710. Fax: +39-011-5644699. E-mail: nunzio.russo@polito.it.

ACKNOWLEDGMENT

M.H. is grateful to the Regione Piemonte and the Politecnico di Torino, Italy for his postdoctoral fellowship grant.

REFERENCES

(1) Saltveit, M. E. Effect of Ethylene on Quality of Fresh Fruits and Vegetables. *Postharvest Biol. Technol.* **1999**, *15*, 279.

(2) Kartheuser, B.; Boonaert, C. Photocatalysis: A Powerful Technology for Cold Storage Applications. *J. Adv. Oxid. Technol.* **2007**, *10*, 107.

(3) Martinez-Romero, D.; Bailen, G.; Serrano, M.; Guillen, F.; Valverde, J. M.; Zapata, P.; Castillo, S.; Valero, D. Tools to Maintain Postharvest Fruit and Vegetable Quality through the Inhibition of Ethylene Action: A Review. *Crit. Rev. Food Sci.* **2007**, *47*, 543.

(4) Maneerat, C.; Hayata, Y.; Egashira, N.; Sakamoto, K.; Hamai, Z.; Kuroyanagi, M. Photocatalytic Reaction of TiO_2 To Decompose Ethylene in Fruit and Vegetable Storage. *Trans. ASAE* **2003**, *46*, 725.

(5) Ye, S.-Y.; Tian, Q.-M.; Song, X.-L.; Luo, S.-C. Photoelectrocatalytic Degradation of Ethylene by a Combination of TiO_2 and Activated Carbon Felts. *J. Photochem. Photobiol., A* **2009**, *208*, 27.

(6) Saltveit, M. E. Is it Possible to Find an Optimal Controlled Atmosphere. *Postharvest Biol. Technol.* **2003**, *27*, 3.

(7) Stow, J. R.; Dover, C. J.; Genge, P. M. Control of Ethylene Biosynthesis and Softening in 'Cox's Orange Pippin' Apples during Low-Ethylene, Low-Oxygen Storage. *Postharvest Biol. Technol.* **2000**, *18*, 215.

(8) Vermeiren, L.; Devlieghere, F.; van Beest, M.; de Kruijf, N.; Debevere, J. Developments in the Active Packaging of Foods. *Trends Food Sci. Technol.* **1999**, *10*, 77.

(9) Guzel-Seydim, Z. B.; Greene, A. K.; Seydim, A. C. Use of Ozone in the Food Industry. *Lebensm.−Wiss. Technol. (1968−2004)* **2004**, *37*, 453.

(10) Bailen, G.; Guillen, F.; Castillo, S.; Serrano, M.; Valero, D.; Martinez-Romero, D. Use of Activated Carbon inside Modified Atmosphere Packages To Maintain Tomato Fruit Quality during Cold Storage. *J. Agric. Food Chem.* **2006**, *54*, 2229.

(11) Liu, Z.-X.; Park, J.-N.; Abdi, S. H. R.; Park, S.-K.; Park, Y.-K.; Lee, C. W. Nano-Sized Carbon Hollow Spheres for Abatement of Ethylene. *Top. Catal.* **2006**, *39*, 221.

(12) Terry, L. A.; Ilkenhans, T.; Poulston, S.; Rowsell, L.; Smith, A. W. J. Development of New Palladium-Promoted Ethylene Scavenger. *Postharvest Biol. Technol.*. **2007**, *45*, 214.

(13) Kim, J.-O. Degradation of Benzene and Ethylene in Biofilters. *Process Biochem.* **2003**, *39*, 447.

(14) Peral, J.; Domenech, X.; Ollis, D. F. Heterogeneous Photocatalysis for Purification, Decontamination and Deodorization of Air. *J. Chem. Technol. Biotechnol.* **1997**, *70*, 117.

(15) Bhatkhande, D. S.; Pangarkar, V. G.; Beenackers, A. A. C. M. Photocatalytic Degradation for Environmental Applications—A Review. *J. Chem. Technol. Biotechnol.* **2001**, *77*, 102.

(16) Hussain, M.; Ceccarelli, R.; Marchisio, D. L.; Fino, D.; Russo, N.; Geobaldo, F. Synthesis, Characterization, and Photocatalytic Application of Novel TiO_2 Nanoparticles. *Chem. Eng. J.* **2010**, *157*, 45.

(17) Guo, J.; Mao, L.; Zhang, J.; Feng, C. Role of Cl^- Ions in Photooxidation of Propylene on TiO_2 Surface. *Appl. Surf. Sci.* **2010**, *256*, 2132.

(18) Yu, H.; Zhang, K.; Rossi, C. Theoretical Study on Photocatalytic Oxidation of VOCs using Nano-TiO_2 Photocatalyst. *J. Photochem. Photobiol., A* **2007**, *188*, 65.

(19) Yamazaki, S.; Tanaka, S.; Tsukamoto, H. Kinetic Studies of Oxidation of Ethylene over a TiO_2 Photocatalyst. *J. Photochem. Photobiol., A* **1999**, *121*, 55.

(20) Zorn, M.; Tompkins, D. T.; Zeltner, W. A.; Anderson, M. A. Catalytic and Photocatalytic Oxidation of Ethylene on Titania-Based Thin Films. *Environ. Sci. Technol.* **2000**, *34*, 5206.

(21) Kumar, P. M.; Badrinarayanan, S.; Sastry, M. Nanocrystalline TiO_2 Studied by Optical, FTIR and X-ray Photoelectron Spectroscopy: Correlation to Presence of Surface States. *Thin Solid Films* **2000**, *358*, 122.

(22) Hou, Y. D.; Wang, X. C.; Wu, L.; Chen, Z. X.; Ding, X. X.; Fu, X. Z. N-Doped SiO_2/TiO_2 Mesoporous Nanoparticles with Enhanced Photocatalytic Activity under Visible-Light Irradiation. *Chemosphere* **2008**, *72*, 414.

(23) Toma, F.-L.; Bertrand, G.; Begin, S.; Meunier, C.; Barres, O.; Klein, D.; Coddet, C. Microstructure and Environmental Functionalities of TiO_2-Supported Photocatalysts Obtained by Suspension Plasma Spraying. *Appl. Catal., B* **2006**, *68*, 74.

(24) Fang, X.; Zhang, Z.; Chen, Q.; Ji, H.; Gao, X. Dependence of Nitrogen Doping on TiO_2 Precursor Annealed under NH_3 Flow. *J. Solid State Chem.* **2007**, *180*, 1325.

(25) Xu, Z.; Shang, J.; Liu, C.; Kang, C.; Guo, H.; Du, Y. The Preparation and Characterization of TiO_2 Ultrafine Particles. *Mater. Sci. Eng.* **1999**, *B56*, 211.

(26) Suriye, K.; Praserthdam, P.; Jongsomjit, B. Control of Ti^{3+} Surface Defect on TiO_2 Nanocrystal using Various Calcination Atmospheres as the First Step for Surface Defect Creation and Its Application in Photocatalysis. *Appl. Surf. Sci.* **2007**, *253*, 3849.